SAPP XXV

25th Symposium on Application of Plasma Processes
and
14th EU-Japan Joint Symposium on Plasma Processing

Book of Contributed Papers

Štrbské Pleso, Slovakia

31 Jan - 5 Feb, 2025

Edited by G. D. Megersa, E. Maťaš, J. Országh, P. Papp, Š. Matejčík

Book of Contributed Papers: 25th Symposium on Application of Plasma Processes and 14th EU-Japan Joint Symposium on Plasma Processing, Štrbské Pleso, Slovakia, 31 January – 5 February 2025.

Symposium organised by Department of Experimental Physics, Faculty of Mathematics, Physics and Informatics, Comenius University in Bratislava and Society for Plasma Research and Applications in hotel SOREA TRIGAN***.

Editors: G. D. Megersa, E. Maťaš, J. Országh, P. Papp, Š. Matejčík

Publisher: Society for Plasma Research and Applications, Bratislava, Slovakia

Issued: January 2025, Bratislava, first issue

ISBN: 978-80-972179-5-2

URL: https://neon.dpp.fmph.uniba.sk/sapp/

Table of Contents

YOUNG SCIENTISTS' LECTURES

IN-SITU DIAGNOSTIC OF ELECTROSPRAY BY RAMAN LIGHT SHEET MICROSPECTROSCOPY

Mário Janda[1], Kasidapa Polprasarn[2], Pankaj Parek[1], David Pai[2]

[1]*Faculty of mathematics, physics and informatics, Comenius University in Bratislava, Slovakia*
[2]*Laboratoire de Physique des Plasmas, CNRS, Sorbonne Université, École Polytechnique, Institut Polytechnique de Paris, Palaiseau, France*
E-mail: janda1@uniba.sk

Cold atmospheric plasma with aerosol generated by electrospray process presents enormous potential for innovations in agriculture, environmental science, and medicine. However, further research is needed to address the challenges of *in-situ* diagnostics of electrospray aerosol particles exposed to plasma. Here we present a study of an electrospray characterized by *in-situ* Raman light sheet microspectroscopy, with a focus on the detection of NO_3^-.

1. Introduction

Aerosols, comprising tiny solid particles or liquid droplets suspended in gas, play significant roles in various environmental, health, and technological contexts [1]. On the other hand, artificially generated aerosols are utilized in various industries, particularly in healthcare [2]. Still more sustainable aerosol technologies are needed to balance the efficiency with the environmental safety. Plasma-activated aerosol (PAA), often referred to as plasma-activated mist or fog [3], is the combination of cold plasma with micrometric aerosol particles. The extremely high surface/volume ratio of water aerosol microdroplets allows harvesting ultrashort-lived reactive species from plasma that have a relatively small impact in processes generating plasma activated water in batch mode, due to their short depth of penetration. Thus, PAA have been reported to achieve extremely high yields of reactive species production [4].

The number and variety of PAA system configurations are rapidly growing but three common aerosol generator systems are usually used, pneumatic, piezoelectric and electrospray (ES) systems [5]. The production of the aerosol mist usually takes place before its treatment by plasma, except for the case of the electrospray, in which the same needle at high voltage can produce at the same time and location both the droplets and the plasma (e.g. transient spark discharge [6]). When a sufficiently high voltage is applied on the capillary (or nozzle), with a liquid flowing through it, the effective surface tension of the liquid starts to decrease due to the presence of an electric field, causing charge separation inside the liquid. This implies the volume of the forming droplets to decrease. When a critical voltage is reached, the shape of the droplet changes to conical, referred to as a Taylor cone [7]. Finally, a jet emerges from the tip of the Taylor cone and breaks into smaller droplets due to various instabilities. [8, 9].

Combining cold atmospheric plasma with aerosol technology presents enormous potential for innovations in agriculture, environmental science, medicine, and industrial pollution control. However, to fully realize the potential of plasma-aerosol systems, further research is needed to address the challenges of diagnostics, stability, and scale-up. Here we present study of ES by *in-situ* monitoring of the Taylor cone, water filament and microdroplets using Raman light sheet microspectroscopy [10], with a focus on detection of NO_3^-.

2. Experimental setup

Figure 1 shows a schematic of the experimental setup for the generation of the water microdroplets by ES process. The setup consists of a reactor, a water supply unit, a DC high voltage (HV) power supply, and electrical diagnostic tools.

To generate an electrospray, a syringe pump (KD Scientific Legato 110) continuously delivers deionized water (100-500 µl/min) or standard NO_3^- solutions (0.5-25 mM) to the reactor through

a blunt hollow stainless steel needle (nozzle) with an inner diameter of 0.5 mm and an outer diameter of 0.7 mm. The needle, acting as the anode, is connected to an HV power supply (FUG Elektronik) via a 13 MΩ ballast resistor. The applied voltage (6-17 kV) is monitored using a DC HV probe (Agilent N2771A) and the signal is processed by a digital oscilloscope (Rohde & Schwarz RTO2024, 2 GHz bandwidth).
The applied high voltage of positive polarity must exceed 5 kV to generate a sufficiently strong electric field between the tip of the needle (anode) and the grounded wire electrode (cathode) to form the electrospray of charged water microdroplets. The gap between the two electrodes is 16 mm, and the diameter of the grounded stainless steel wire electrode is 2 mm.

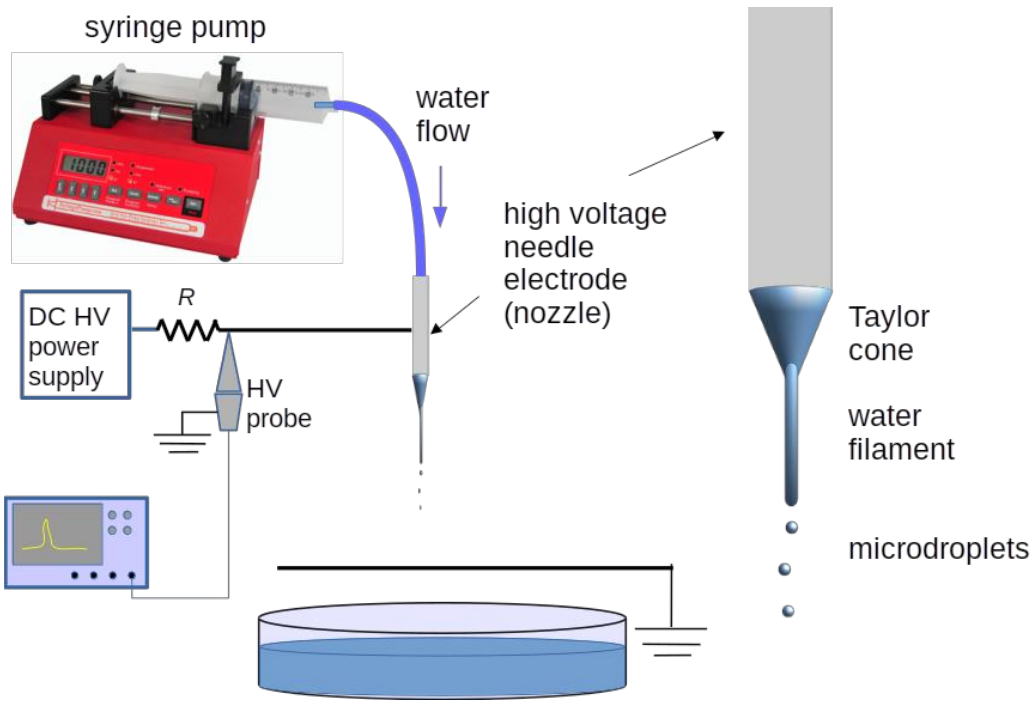

Fig. 1. Simplified schematic of the electrospray setup.

The Raman spectrometer is nearly identical to the system described in Ref. [10]. As shown in Figure 2, a diode-pumped solid-state laser (Elforlight Spot) produced pulses at 532 nm of 2 ns duration at a repetition frequency of 30 kHz, with the average power measured to be 452 mW. The beam first passed through an expander, followed by a variable power attenuator consisting of a rotating half-wave plate combined with a polarizing beamsplitter. The beam underwent vertical focusing upon passing through a cylindrical lens. Upon reflection off a dichroic mirror (Semrock RazorEdge), the beam focused horizontally via a 10X microscope objective (Mitutoyo M Plan Apo and working distance 34 mm). The focus point did not change during the experiments, but the ES reactor was placed on a 3D micrometric positioning system and it was thus possible to focus at different positions below the nozzle.
During in situ measurements, the laser was stable in power to within 3% with a jitter of 1 ns, as measured by a power meter and photodiode placed behind the dichroic mirror. The backscattered light was filtered through the dichroic mirror and then a notch filter (Semrock StopLine). The parallel component of the Raman signal was focused onto the entrance slit of a monochromator (Acton SP2500i, f/6.5 and focal length 0.5 m) coupled with an intensified CCD camera (Princeton Instruments PIMAX 4) mounted at the exit plane of the monochromator.
A delay generator (Stanford Research Systems DG645) synchronized the triggering of the camera gating and the laser. The camera gate duration was 30 ns. Number of accumulations per exposure,

exposures per frame, and camera gain, were adjusted for each measurement to provide and acceptable trade-off between the signal-to-noise ratio and acquisition time.
An additional Tungsten lamp or a LED lamp was used to visualize the target using a CMOS camera (Zelux 1.6 MP Color) during the alignment process. For the alignment we used a cw laser (Laser Quantum Gem).

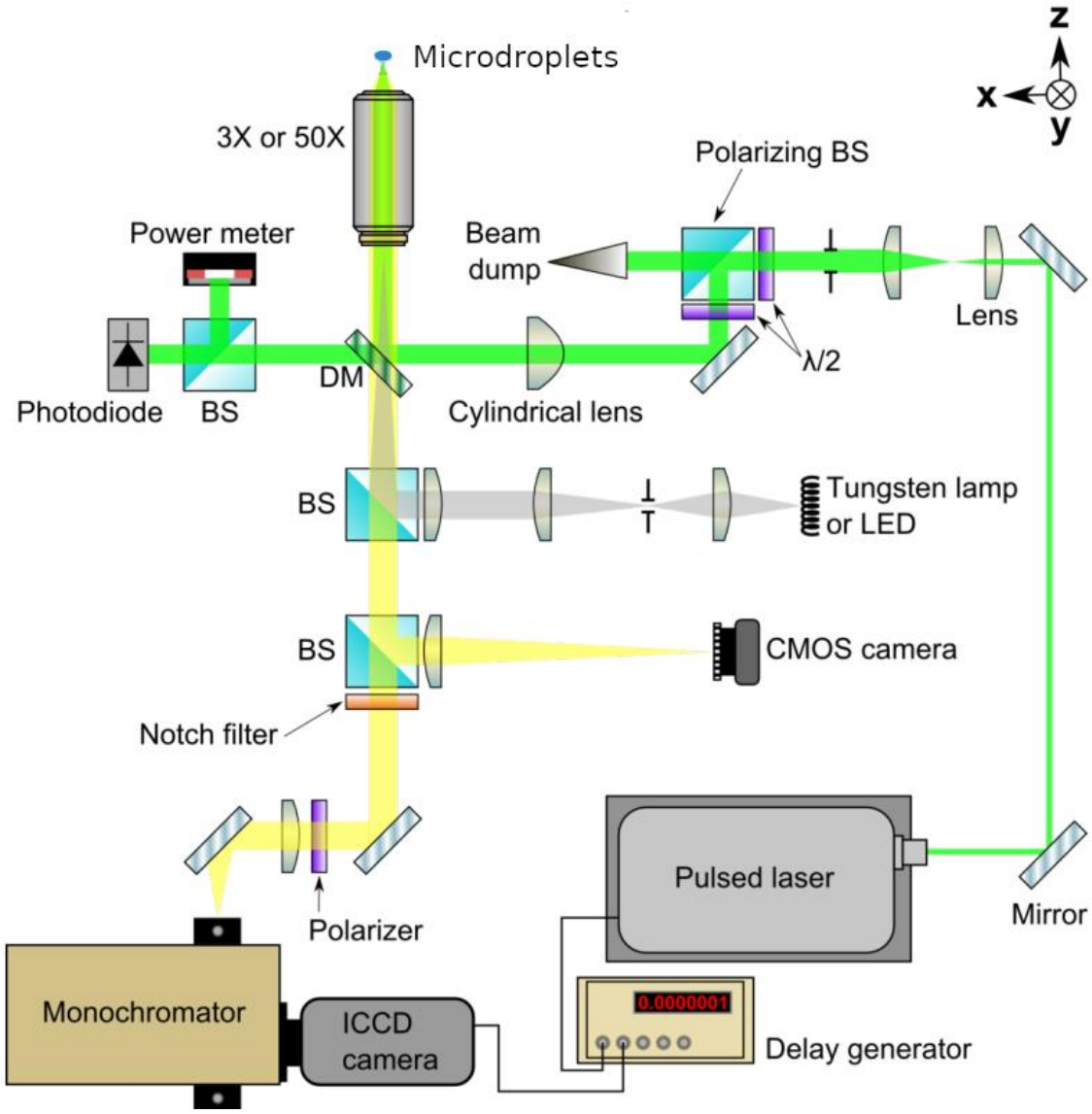

Fig. 2. Top-view schematic diagram of the in situ Raman microspectrometer. The abbreviations are as follows: half-wave plates (λ/2), beamsplitters (BS), dichroic mirror (DM).

3. Results and Discussion

A 3D micrometric positioning system enabled us to focus the laser beam at different positions below the nozzle. Thus we were able to test the possibility of getting Raman signal from all three stages of the electrospray: the Taylor cone, filament and microdroplets (depicted on Figure 1). As an example, Figure 3 shows a camera image of the ES water filament with the reflection from the cw laser used for alignment (green color). We used the objective with 10x magnification, and the area of the camera chip is 4.95 x 3.33 mm (1440x1080 pixels). Based on these numbers, the estimated width of the water filament, as indicated in Figure 3, is approximately 130 µm.

At an applied voltage of 6.5 kV (6 kV at the needle), we obtained a relatively stable ES mode, and thus also relatively stable reflection and backscattering of the laser beam. We were able to record Raman spectra with good signal to noise ratio from both the Taylor cone and from the water filament formed below the Taylor cone. Further away, where the filament disintegrates into microdroples, the signal decreases significantly. Figure 4 shows the decrease of Raman signal intensity as a function of distance from the end of the Taylor cone.

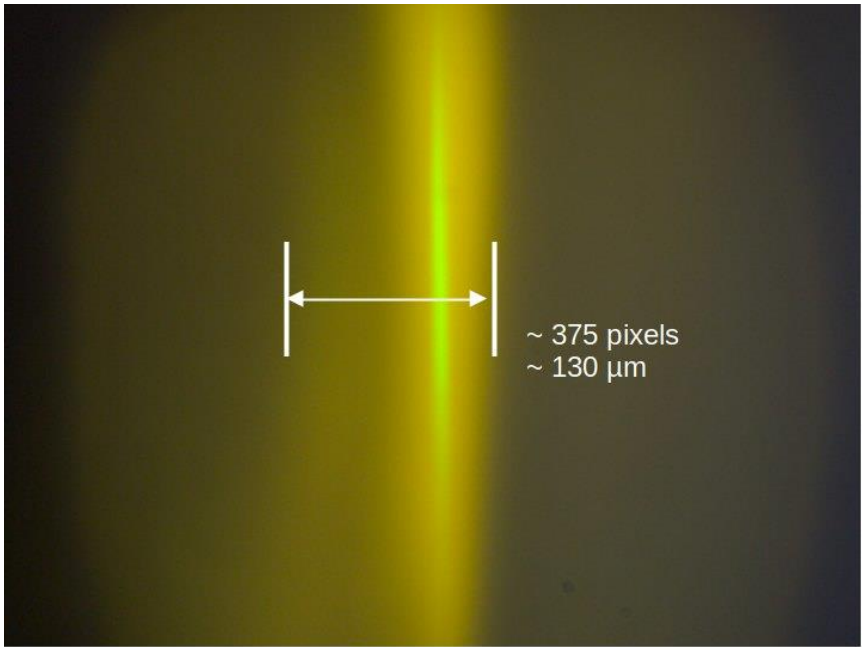

Fig. 3. A camera image of ES water filament with reflection of alignment cw laser (green color), water flow rate of 300 µl/min, applied voltage of 6.5 kV (6 kV at the needle, as measured by HV probe).

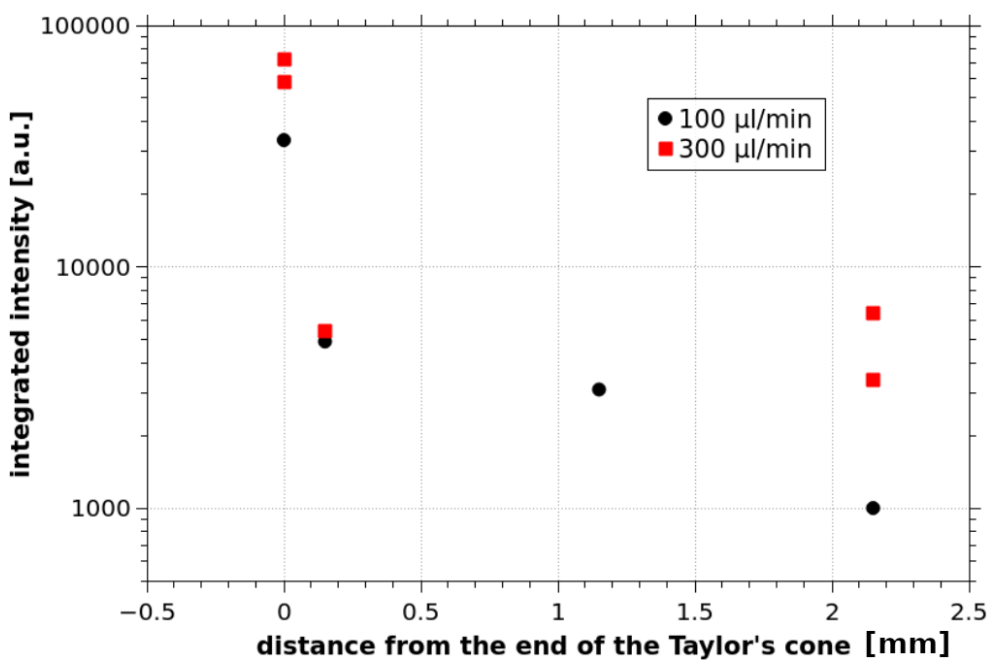

Fig. 4. Integrated intensity of the Raman signal (scattering by H_2O, wavenumbers 2600-4000 cm^{-1}) as a function of the measurement position, two different water flow rates.

The signal in Figure 4 is integrated over the wavenumbers 2600-4000 cm^{-1} corresponding to the Raman scattering by H_2O molecules (-OH stretch). Note that the formation (dripping) of microdroplets from the filament is not synchronized with the laser pulses. Moreover, the formed microdroplets do not follow the same path and only some of them can interact with the laser beam. This can explain significant decrease of the signal further away from the Taylor cone, in the zone of microdroplets.

Despite this fact, it was possible to obtain Raman spectra also from light scattered by the micdrodroplets, and it was even possible to see peak corresponding to the NO_3^- symmetric stretch mode near 1050 cm^{-1}. Figure 5 shows normalized background corrected Raman spectra of 5 mM NO_3^- solution, measured at three different positions (Taylor cone, filament, droplets). With normalization, it is possible to see different S/N when measuring at three different positions. In the case of spectra measured at the Taylor cone or in the filament, the NO_3^- peak is well visible and the detection limit is probably around concentration of 1 mM. In the case of the signal from droplets, the NO_3^- peak is also visible, but it is comparable to the noise level.

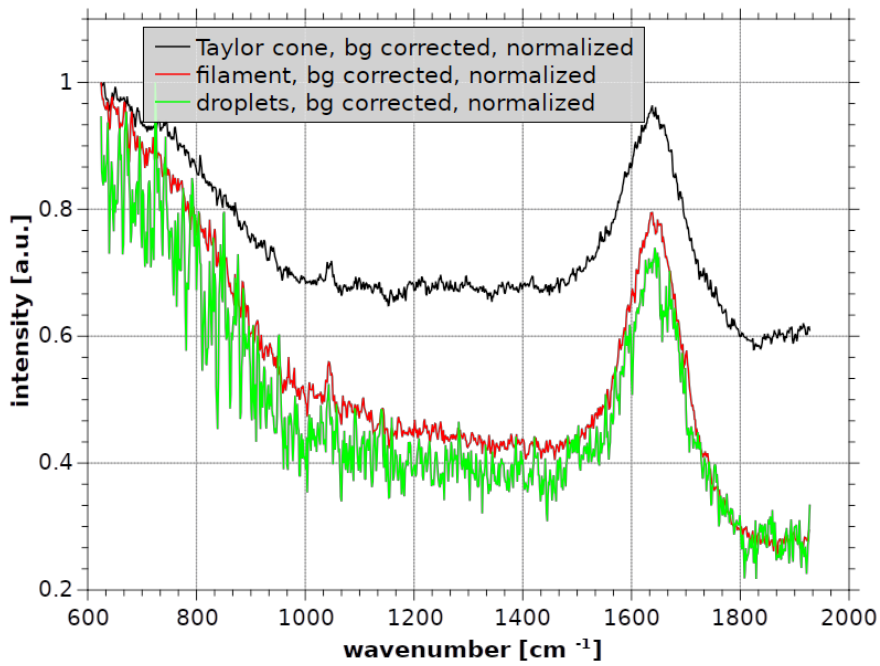

Fig.5. Normalized Raman spectra measured at three different positions, water flow rate of 300 µl/min, 6 kV at the needle, 5 mM NO_3^- solution.

4. Conclusions

We have shown that *in-situ* monitoring of the Taylor cone, water filament and microdroplets by using Raman light sheet microspectroscopy is possible. This technique can be also used to monitor NO_3^- in ES microdroplets. However, the detection limit needs to be improved from about 1-5 mM to much lower values, so that this technique can be used for probing the gradual increase of the NO_3^- in the microdroplets exposed to the plasma. This could be probably achieved by using the coherent anti-Stokes Raman scattering technique.

Acknowledgment: Funded by the EU NextGenerationEU through the Recovery and Resilience Plan for Slovakia under the project No. 09I03-03-V03-00033 EnvAdwice, and by APVV Agency bilateral grant SK-FR-22-0014.

5. References

[1] Anlimah, F, Gopaldasani V, MacPhail C and Davies B 2023 *Environ Sci Pollut Res* **30** 54407–54428.
[2] Rogliani P et al. 2017 *Respiratory Medicine* **124** 6–14.
[3] Aceto, D et al. 2024 Atmospheric Pressure, Low Temperature Plasma applications for decontamination of agrifood products, ESCAMPIG XXVI, Brno, Czech Republic, July 9–13.
[4] Locke B R and Shih K-Y 2011 *Plasma Sources Sci. Technol* **20** 034006.
[5] Janda M, Stancampiano A, di Natale F and Machala Z 2024 Short Review on Plasma-Aerosol Interactions, *Plasma Process. Polym.,* e2400275. https://doi.org/10.1002/ppap.202400275
[6] Machala Z et al. 2013 *Plasma Process. Polym.* **10** 649–659.
[7] Taylor G 1964 *Proc. R. Soc. Lond. A* **280** 383–97
[8] Cloupeau M and Prunet-Foch B 1990 *J. Electrostat.* **25** 165–84
[9] Hartman R P A et al. 2000 *J. Aerosol Sci.* **31** 65-95.
[10] Pai D Z 2021 *J. Phys. D: Appl. Phys.* **54** 355201.